

1 **Fluency shaping increases integration of the command-to-execution and the auditory-to-motor**
2 **pathways in persistent developmental stuttering**

3

4 Alexandra Korzeczek^{a,#}, Annika Primaßin^{a,b#}, Alexander Wolff von Gudenberg^c, Peter Dechent^d,
5 Walter Paulus^a, Martin Sommer^{a,e,f}, and Nicole E. Neef^{f,a,g*}

6

7 ^aDepartment of Clinical Neurophysiology, University Medical Center Göttingen, Göttingen, Germany

8 ^bFH Münster University of Applied Sciences, Münster School of Health (MSH), Münster, Germany

9 ^cInstitut der Kasseler Stottertherapie, Bad Emstal, Germany

10 ^dMR Research in Neurology and Psychiatry, Department of Cognitive Neurology, University Medical
11 Center Göttingen, Göttingen, Germany

12 ^eDepartment of Neurology, University Medical Center Göttingen, Germany

13 ^fDepartment of Geriatrics, University Medical Center Göttingen, Germany

14 ^gDepartment of Diagnostic and Interventional Neuroradiology, University Medical Center Göttingen,
15 Göttingen, Germany

16

17 **#These authors contributed equally**

18 ***Correspondence:** Nicole E. Neef, Department of Diagnostic and Interventional Neuroradiology

19 University Medical Center, Georg August University, Robert-Koch-Straße 40, 37075 Göttingen,

20 Germany, nneef@gwdg.de

21 **Contacts:** Alexandra Korzeczek alexandra.kore@posteo.de; Annika Primaßin [22 \[muenster.de\]\(mailto:muenster.de\); Alexander Wolff von Gudenberg \[awvgudenberg@kasseler-stottertherapie.de\]\(mailto:awvgudenberg@kasseler-stottertherapie.de\); Peter](mailto:annika.primassin@fh-</p></div><div data-bbox=)

23 Dechent Peter.Dechent@medizin.uni-goettingen.de; Walter Paulus [24 \[goettingen.de\]\(mailto:goettingen.de\); Martin Sommer \[martin.sommer@med.uni-goettingen.de\]\(mailto:martin.sommer@med.uni-goettingen.de\)](mailto:wpaulus@med.uni-</p></div><div data-bbox=)

25

26 **Running title:** Sensorimotor plasticity in stuttering

27

28 **Abstract**

29 Fluency-shaping enhances the speech fluency of persons who stutter, yet underlying conditions and
30 neuroplasticity-related mechanisms are largely unknown. While speech production-related brain
31 activity in stuttering is well studied, it is unclear whether therapy repairs networks of altered
32 sensorimotor integration, imprecise neural timing and sequencing, faulty error monitoring, or
33 insufficient speech planning. Here, we tested the impact of one-year fluency-shaping therapy on
34 resting-state fMRI connectivity within sets of brain regions subserving these speech functions. We
35 analyzed resting-state data of 22 patients who participated in a fluency-shaping program, 18 patients
36 not participating in therapy, and 28 fluent control participants, measured one year apart. Improved
37 fluency was accompanied by an increased synchronization within the sensorimotor integration
38 network. Specifically, two connections were strengthened; the left inferior frontal gyrus showed
39 increased connectivity with the precentral gyrus at the representation of the left laryngeal motor
40 cortex, and the left inferior frontal gyrus showed increased connectivity with the right superior
41 temporal gyrus. Thus, therapy-associated neural remediation was based on a strengthened
42 integration of the command-to-execution pathway together with an increased auditory-to-motor
43 coupling. Since we investigated task-free brain activity, we assume that our findings are not biased to
44 network activity involved in compensation but represent long-term focal neuroplasticity effects.

45

46 **Keywords**

47 stuttering intervention, sensorimotor integration, neuroplasticity, inferior frontal gyrus, dorsal
48 laryngeal motor cortex

49

50 Introduction

51 Most people speak fluently with ease, but fluent speech requires a complex interplay across multiple
52 functional domains. In stuttering, aberrant brain activity and connectivity is evident in networks that
53 convey fluent speech production (Ingham et al., 2018). However, especially in adults who
54 experienced lifelong stuttering, it is challenging to differentiate core neural deficits from stuttering-
55 induced neural signatures or intervention-induced neuroplasticity from compensatory network
56 activity (Kell, 2012). Thus, our understanding of the neurophysiological mechanistic principles of
57 stuttering and its neural remediation remains limited.

58 The neural networks that may become involved during stuttering intervention have hardly been
59 studied. Previous neuroimaging studies reported local and distributed intervention-induced activity
60 changes in the left inferior frontal gyrus (Kell et al., 2009; Lu et al., 2017; Neumann et al., 2018),
61 cerebellum (De Nil et al., 2001; Lu et al., 2012; Toyomura et al., 2015), and basal ganglia (Toyomura
62 et al., 2015), and a change in lateralization of speech-related frontal brain activity towards the more
63 typical leftwards pattern (De Nil et al., 2003; Kell et al., 2009; Neumann et al., 2018, 2003). All except
64 one earlier study (Toyomura et al., 2015) involved the training of voicing patterns to shape speech
65 fluency, a common approach to overcome stuttering.

66 Fluency shaping is a speech restructuring method that requires individuals to change their speech
67 patterns. Specifically, during fluency shaping, patients learn to speak slowly with gentle onsets of
68 phonation, light articulatory contacts, and soft voicing of plosives (Euler et al., 2009; Webster, 1974).
69 After three weeks of fluency shaping training, connectivity was increased between the left anterior
70 superior temporal gyrus and the left articulatory motor cortex, and hyperconnectivity was reduced
71 between the left IFG pars opercularis and the sensory feedback processing left supramarginal gyrus
72 (Kell et al., 2018). This observation suggests a treatment-induced boost of auditory-to-motor
73 coupling and likely indicates neuroplasticity induced by sensorimotor learning (Calmels, 2020).
74 However, a stuttering intervention that leads to a significant reduction of speech dysfluencies in
75 adults (Euler et al., 2009) and children (Euler et al., 2021) presumably addresses large-scale

76 functional networks that exceed auditory-to-motor mapping. Further supporting domains that are
77 related to speech processing could be speech planning (Andreatta et al., 2010; Price, 2012),
78 sensorimotor integration (Behroozmand et al., 2015; Darainy et al., 2019; Hickok et al., 2011;
79 Tourville et al., 2008), articulatory convergence (Brown et al., 2005; Guenther, 2016; Turkeltaub et
80 al., 2002), and the inhibition of competitive processes (Ghahremani et al., 2018; Xue et al., 2008).
81 Previous studies might have failed to detect changes in these crucial functional domains because
82 measured brain activity was biased by the tasks employed.

83 One suitable approach to scrutinizing learning-induced neuroplasticity is resting-state functional
84 magnetic resonance imaging (rs-fMRI). On the one hand, rs-fMRI is free from confounds of task
85 performance, particularly in participants who may present symptoms such as physical concomitants
86 during speaking. Thus, task-free brain activity assesses changes in brain dynamics that are not biased
87 by differences in how a task is performed in pre-learning versus post-learning condition (Vahdat et
88 al., 2011). On the other hand, it is widely assumed that ongoing spontaneous global activity of the
89 brain at rest is (1) highly-structured, (2) closely relates to underlying anatomical connectivity, and (3)
90 reflects local neuronal dynamics, signal transmission delay, and genuine noise, i.e., unstructured
91 input (Deco et al., 2011). It has been shown that even under the resting-state condition, brain areas
92 show activity changes with learning, and correlated activity increases between learning-related areas
93 (Albert et al., 2009; Darainy et al., 2019; Vahdat et al., 2011).

94 To date, task-free brain activity has been studied twice to test stuttering intervention-induced
95 neuroplasticity (Lu et al., 2017, 2012). Both studies investigated the same speech therapy. During the
96 7-day intervention with three daily sessions, participants trained a new voicing pattern with word
97 listen-and-repeat tasks followed by overt-Pinyin-reading tasks. Later, participants listened to their
98 audio-recordings and received the therapist's feedback. In addition, participants applied the newly
99 learned speaking pattern to utterances produced throughout their daily lives (Lu et al., 2017). The
100 first study showed an intervention-related decrease of rs-fMRI connectivity in the left declive and
101 vermis area of the cerebellum. In addition, connectivity changes in the cerebellum correlated

102 positively with the change of stuttering severity after the change of duration of the stuttering events
103 and physical concomitants was regressed out (Lu et al., 2012). Because stuttering-related cerebellar
104 overactivity was often considered to reflect compensatory activity (Brown et al., 2005; De Nil et al.,
105 2008; Lu et al., 2010; Watkins et al., 2008), Lu and colleagues suggested the reduced cerebellar rs-
106 fMRI connectivity to display reduced compensatory activity and, thus, to indicate a neural
107 reorganization of the intrinsic functional architecture of speech processing. The second study, which
108 included a reduced number of the same participants, showed that rest-related connectivity changes
109 in the cerebellum and task-related activity increases in the left ventral inferior frontal gyrus and
110 insula, were not correlated. The task-related activity was measured during the overt reading of
111 monosyllabic Chinese characters (Lu et al., 2017). This observation was discussed to support the idea
112 that resting-state functional connectivity and task-related brain activity provide different insights into
113 mechanisms behind brain plasticity.

114 Here, we use a longitudinal approach to examine stuttering intervention-induced improvement in
115 speech fluency and neurofunctional reorganization. To this end, we acquired rs-fMRI data before and
116 11 months after a computer-assisted fluency shaping training (Euler et al., 2009) in persons with
117 developmental stuttering (PDS+) and tested time-dependent connectivity changes. We controlled for
118 the specificity of intervention-induced changes by studying two control groups, i.e., patients with
119 developmental stuttering not taking part in any stuttering intervention (PDS-) and fluent controls
120 (FC). We quantified the synchronicity of spontaneous low-frequency fluctuations to characterize the
121 connectivity between functionally related brain hubs. We determined sets of ROIs to assess
122 connectivity of *a priori* determined semi-discrete networks associated with speech planning (Bohland
123 and Guenther, 2006; Rottschy et al., 2012), articulatory convergence (Guenther, 2016), speech-
124 related sensorimotor integration (Darainy et al., 2019), and speech motor inhibitory control
125 (Ghahremani et al., 2018; Neef et al., 2016). All ROIs were chosen from the literature. However, we
126 made no directional hypothesis before the data collection. Chosen ROIs capture spontaneous BOLD
127 fMRI fluctuations of neuronal populations that are integral parts of brain networks. Network

128 dynamics are without much doubt nonlinear and difficult to predict. In this vein, the outcomes were
129 not predicted and are therefore exploratory. To capture brain-behavior relationships, we additionally
130 explored correlations between changes in functional connectivity and speech fluency.

131

132 **Methods**

133 *Participants*

134 The current data were collected during a dissertation project (Primaßin, 2019) that evaluated the
135 long-term effects of an intensive stuttering intervention on white matter integrity and task-related
136 brain activity. Persons who stutter who were about to begin with intervention at the Kassel
137 Stuttering Therapy (KST) were invited to participate in the MRI study. Volunteers from the KST were
138 assigned to PDS+. Fluent control participants were recruited via advertisements at the homepage of
139 the Department of Clinical Neurophysiology and at notice boards of the university campus and clinic
140 and were assigned to FC. Stuttering controls were recruited via announcements at stuttering self-
141 help groups and at the 2016 annual congress of the German stuttering self-help group association
142 (BVSS). Stuttering controls did not participate in any stuttering intervention during the entire study
143 period and were assigned to PDS-.

144 Seventy-six right-handed, monolingual speakers of German participated voluntarily in the current
145 study. Exclusion criteria were speech or language disorders other than developmental stuttering,
146 neurological impairment, drug abuse, or medications that act on the central nervous system. None of
147 the PDS- took part in any stuttering intervention during the entire study period. For analysis, we
148 excluded the data of three PDS+ because they participated in addition in a different stuttering
149 intervention. Data of further four participants (1 PDS+, 2 PDS-, 1 FC) were excluded because of
150 missing behavioral or rs-fMRI data, and data of one PDS+ were excluded because of extensive rs-fMRI
151 motion artifacts. Thus, the rs-fMRI data analysis comprised 22 PDS+ (2 females, mean age 25.6 ± 11.7
152 years with 7 participants younger than 18 years), 18 PDS- (2 females, mean age 34.8 ± 7.0 years, with

153 no participant younger than 18 years), and 28 FC (4 females, mean age 25.1 ± 7.4 years with 5
 154 participants younger than 18 years). While age was comparable between PDS+ and FC with $T = -0.16$
 155 and $p = 0.87$, PDS+ were younger than PDS- with $T = -3.1$ and $p = 0.004$, and PDS+ were younger than
 156 PDS- with $T = -4.49$ and $p < 0.001$. PDS+ and FC were matched with regard to sex and handedness
 157 (Oldfield, 1971). PDS- had a higher education score than participants in the two other groups (see
 158 Table 1). Speech fluency (Stuttering severity index, SSI-4) (Riley et al., 2004) of all participants was
 159 assessed prior to each MRI session. Stuttering severity was lower in PDS- than in PDS+ (Table 1). In
 160 addition, a self-assessment of the psychosocial impact of stuttering (Overall Assessment of the
 161 Speaker's Experience of Stuttering, OASES) (Yaruss and Quesal, 2014) indicated that PDS+ were more
 162 affected by stuttering than PDS-. Finally, both PDS- and PDS+ were comparable regarding the time
 163 span in years that had passed since the last stuttering intervention before participating in the current
 164 study (Table 1 and Supplementary Table 1). There were three participants per group not providing
 165 information on their stuttering intervention history. Age of intervention and nature of intervention
 166 varied in both groups. However, the groups were too small to compare them with respect to these
 167 two variables.

168

169 **Table 1 Demographic data of participants**

	PDS+	PDS-	FC	Test-statistics (<i>df</i>)	two-sided <i>p</i> -value
<i>n</i>	22	18	28		
Age, years	25.6 ± 11.7	$34.8 \pm 7.0^*$	25.1 ± 7.4	$7.58 (2, 65)^i$	0.001
Sex ratio	20:2	16:2	24:4	– ⁱⁱ	0.89
Education ^a	2 (1.0) ⁻	6 (3.0)*	3 (2.8)	$16.68 (2,68)^{iii}$	< 0.001

Handedness	91 (12)	91 (33)	100 (33)	0.04 (2,68) ⁱⁱⁱ	0.98
SSI-4 at T1	25 (14.3) [#]	14 (11.3)	–	2.56 ^{iv}	0.010
SSI-4 at T2	9 (10.5)	12.5 (11.0)	–	-1.31 ^{iv}	0.194
OASES at T1	3.0 (0.6) [#]	2.0 (0.4)	–	4.70 ^{iv}	< 0.001
OASES at T2	1.9 (0.5)	2.0 (0.5)	–	-0.65 ^{iv}	0.516
Last therapy, years ago	8.5 ± 8.7 [~]	12.7 ± 8.8 [~]		-1.18(32) ^v	0.249
Onset, years	4.8 ± 3.0	5.0 ± 3.6	–	0.22 ^{iv}	0.839
MRI interval, months	11.6 ± 1.0	11.6 ± 1.4	11.4 ± 0.8	0.95 (2) ⁱⁱⁱ	0.623

170 *Interval/ratio -scaled variables are presented as mean ± standard deviation. Ordinal-scaled variables*
 171 *are presented as median (interquartile range). *significantly different from both other groups in post*
 172 *hoc comparisons (p < 0.001), #significantly different from stuttering controls (p < 0.001), ~ three*
 173 *missing values, ⁱone-way independent ANOVA, ⁱⁱFisher's exact test, ⁱⁱⁱKruskal-Wallis test, ^{iv}Mann-*
 174 *Whitney test, ^vunpaired t-test, ^aachieved education levels were 1 = still attending school, 2 = school, 3*
 175 *= high school, 4 = <2years college, 5 = 2 years of college, 6 = 4 years of college, 7 = postgraduate*

176

177 The study was registered on January 14, 2016, at the study center of the University Medical Center of
 178 Göttingen and was given the registration number 01703. This registration is not publicly accessible,
 179 but access could be requested under the following email address: sz-umg.registrierung@med.uni-
 180 goettingen.de. The ethical review board of the University Medical Center Göttingen, Georg August
 181 University Göttingen, Germany, approved the study, and all participants gave their written informed
 182 consent, according to the Declaration of Helsinki, before participation. In addition, informed consent
 183 was obtained from parents or legal guardians of participants under the age of 18.

184 All participants took part in two MRI sessions (T1 and T2) separated by 10 to 15 months. The
185 scanning interval was similar between groups (Table 1). PDS+ were scanned pre- (T1) and post-
186 intervention (T2).

187 *Intensive stuttering intervention and follow-up care*

188 PDS+ took part in the Kasseler Stottertherapie (Euler et al., 2009), an intensive program that
189 incorporates fluency shaping with computer-assisted biofeedback during a two-week on-site and
190 one-year follow-up treatment. Fluency shaping reconstructs patterns of vocalization, articulation,
191 and respiration, resulting in prolonged speech, soft voice onsets of initial phonemes, and a smooth
192 transition between sounds. It was first introduced with the precision fluency shaping program by
193 Webster (Max Ludo and Caruso Anthony J., 1997; Webster, 1980, 1974). The overarching aim of this
194 approach is to train to speak slowly with gentle onsets of phonation, light articulatory contacts, and
195 soft voicing of plosives. In the current study, the on-site intervention encompassed two weeks of
196 intensive therapy and training, i.e., at least eight hours per day and seven days per week. The
197 intervention was structured into alternating sessions. Sessions included group therapy, individual
198 computer-assisted speech training, one-to-one speech therapy, and in-vivo training. In-vivo training
199 stands for applying the speech technique in real-life situations that require patients to talk to persons
200 outside the therapy setting while still receiving support from a therapist. Next to applying the speech
201 technique during everyday communication, participants were encouraged to practice daily with the
202 computer. Computer-assisted training at home was mainly based on the biofeedback-assisted
203 practice of the new speech patterns. Biofeedback consisted of a visualization of the speech sound
204 wave. As an incentive, participants could get the costs of the software reimbursed by their health
205 insurance if they practiced at least 1980 minutes within the first half of the year and 990 minutes
206 within the second half (Euler et al., 2009). Thus, the intervention under study was the same as in Kell
207 et al. (2018, 2009) and Neumann et al. (2018, 2005, 2003), differed in the way of providing feedback
208 from the one in De Nil et al. (2003) and differed in intervention duration, therapy content, and
209 provision of feedback from the stuttering intervention studied in the only other resting-state study

210 (Lu et al., 2017, 2012). During the follow-up period, there were two refresher courses at the therapy
211 center at one month and ten months, respectively, after the initial intensive training. If participants
212 were not able to attend the 10-month refresher, they could also attend subsequently offered
213 refresher courses. In this study, participants scheduled the second refresher at the latest 14 months
214 after the intervention. On rare occasions, due to organizational issues, MRI measurements at T2 took
215 place one day before the second refresher.

216

217 *Assessment and statistical analysis of behavioral data*

218 Changes in speech fluency were assessed by two experienced speech-language pathologists (one of
219 whom was A.P.) using the Stuttering Severity Index (SSI-4). The SSI-4 assessment included a
220 spontaneous speech sample and a reading sample. Each sample comprised 488 to 500 syllables. For
221 interrater reliability estimation, the two raters analyzed nine randomly chosen participants, three
222 from each group. Reliability estimates were statistically assessed with SPSS software with
223 Krippendorff's Alpha Reliability Estimate (KALPHA) using 10,000 bootstrapping samples at an ordinal
224 level (Hayes and Krippendorff, 2017). KALPHA ranged between 0.84 and 0.98 for the SSI-4 sub-scores
225 reading, spontaneous speech, duration, and concomitants. KALPHA was 0.96 for the SSI-4 total score,
226 indicating a good to excellent consensus between raters. The participants' experience with stuttering
227 was assessed with the German version of the OASES (Yaruss and Quesal, 2014). We assessed
228 behavioral changes as a change in the SSI-4 total scores and change in the OASES total scores
229 between T1 and T2 using R (version 3.5.3). We ran robust mixed ANOVAs on trimmed means with
230 Group as between-factor and Time as within-factor using the function *tsplit* with the default
231 trimming level of 0.2 of the package WRS (R.R. Wilcox' robust statistics functions -version 0.37). Time
232 was implemented as the second factor. Post hoc we applied Wilcoxon signed-rank tests.

233

234 *Definition of four speech-related semi-discrete brain networks*

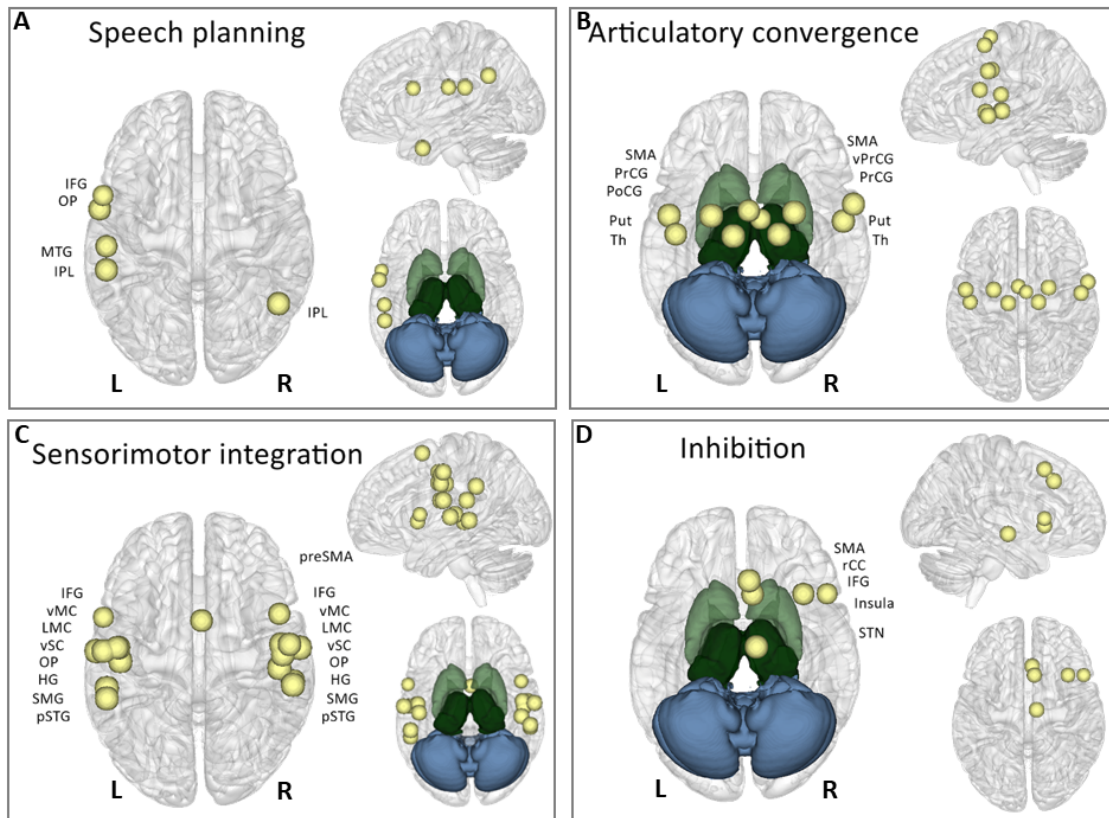
235 Resting-state fMRI captures brain activity in the absence of a task. Spontaneous fluctuations of the
236 blood-oxygen-level-dependent (BOLD) signal represent specific patterns of synchronous activity and
237 reflect the functional organization of the brain (Biswal et al., 1995). Compared to data-driven
238 approaches, which are also common to study rs-fMRI activity, ROI-to-ROI analyses provide detailed
239 information on the specific connectivity of brain areas of interest as demonstrated for the dorsal and
240 ventral attentional systems (Fox et al., 2006) or the functional connectivity of the anterior cingulate
241 cortex (Margulies et al., 2007). Fluent speech production engages large-scale brain networks
242 conveying emotional, linguistic, cognitive, sensory, and motor functions. Among these processes,
243 dysfunctional speech planning, articulatory convergence, sensorimotor integration or motor
244 inhibition most likely cause the primary motor signs of stuttering, which are sound and syllable
245 repetitions, sound prolongations, and speech blocks. Here, we distinguished four semi-discrete brain
246 networks consisting of brain regions that are recruited for any of these functions (Fig. 1).

247 Several left-hemispheric regions contribute to speech planning: posterior inferior gyrus, insula,
248 temporoparietal regions, and the proper and pre-supplementary motor area (Andreatta et al., 2010;
249 Price, 2012). A selected brain region of dysfunctional *speech planning* was derived from a fixed-
250 effects analysis of an earlier fMRI study of our lab that investigated imagined speaking compared
251 with humming in 15 PDS and 15 FC (Neef et al., 2016) (Fig. 1A). Between-group contrasts of an ROI
252 analysis within the area BA 44 and of a functional connectivity analysis with the left posterior area 44
253 as seed revealed dysfunctional brain regions of speech planning in PDS (Neef et al., 2016).

254 *Articulatory convergence* seeds originated from combined ALE meta-analyses (Guenther, 2016) on
255 brain imaging studies of simple articulatory movements of the jaw, larynx, lips, tongue, and
256 respiratory system (Fig. 1B). The rationale behind this concept was that speaking requires the joint
257 coordination of multiple articulatory subsystems, i.e., jaw movements, lip movements, larynx
258 movements, respiratory movements, and tongue movements. Brain regions that are involved in the
259 control of multiple articulatory subsystems were defined as regions of high articulatory convergence.
260 To determine such brain regions, Guenther (2016) performed five activation likelihood estimate (ALE)

261 meta-analyses, one for each subsystem, thereby including only functional imaging contrasts of non-
262 speech movement tasks. Afterward, he identified brain coordinates where foci of three or more
263 articulatory systems showed very close proximity by visual inspection(Guenther, 2016). Speech-
264 related *sensorimotor integration* seeds were derived from a ‘listen-and-repeat’ localizer task in a
265 brain imaging study of sensorimotor plasticity in speech motor adaptation (Darainy et al., 2019) (Fig.
266 1C). The study investigated in 19 neurotypical participants on two consecutive days whether
267 behavioral learning-related changes in perception and speech movements influenced brain motor
268 areas directly or indirectly via sensory areas. ROI-to-ROI analyses of rs-functional connectivity were
269 used to identify sensorimotor plasticity between the first and the second day (Darainy et al., 2019).
270 Of note, the ROI coordinates of the primary motor cortex (mid precentral gyrus) reported by (Darainy
271 et al., 2019) were exchanged because of the differences in speech tasks. Whereas participants in
272 Darainy et al. (2019) adjusted articulatory movements to the perception of vowels, the stuttering
273 intervention required the modification of voicing and thus a skillful control of the larynx. (Neumann
274 et al., 2018) for example reported that the very same stuttering intervention normalized the mean
275 fundamental frequency (meanF0) for PWS+. Thus, coordinates of the laryngeal motor cortex (LMC)
276 that were chosen for replacement, were derived from a fMRI meta-analysis encompassing 19 overt
277 speech production studies with 283 neurotypical participants (Kumar et al., 2016; Simonyan, 2014).
278 For further rs-fMRI analyses in CONN (SPM toolbox), the coordinates in Talairach space, left LMC at [-
279 45, -14, 33] and right LMC at [44, -12, 35], reported by Kumar et al. (2016), were converted with
280 GingerALE (<http://www.brainmap.org/ale/>) using the transform “Talairach to MNI (SPM)” to MNI
281 space, left LMC [-47, -10, 34] and right LMC [49, -8, 35]. *Motor inhibition* seeds that involved common
282 areas of inference resolution, action withholding, and action cancellation were derived from a meta-
283 analysis of 225 studies (Zhang et al., 2017). We added the subthalamic nucleus seed to the inhibition
284 network to account for the dedicated involvement of this structure in response inhibition (Aron and
285 Poldrack, 2006) (Fig. 1D). In two experiments, this study showed the inhibitory role of the
286 subthalamic nucleus using action cancellation tasks (stop-signal task)(Aron and Poldrack, 2006).

287 We created spherical seeds with a radius of 6 mm for all ROIs. Coordinates for brain hubs involved in
 288 speech-related sensorimotor integration can be found in Table 2. Seeds for the remaining three
 289 networks are listed in Supplementary Tables 3-5. Seed ROIs did not overlap.



290

291 **Figure 1 ROI-to-ROI resting state fMRI analyses were conducted in four semi-discrete functional networks.**

292 Spheres with a diameter of 6 mm served as seed regions, overlaid here on rendered surfaces of the MNI
 293 standard brain. Intervention effects were tested for speech planning (A), articulatory convergence (B),
 294 sensorimotor integration (C), and motor inhibition (D). HG = Heschl's gyrus, primary auditory cortex; IPL =
 295 inferior parietal lobe; IFG = inferior frontal gyrus, pars opercularis; LMC = laryngeal motor cortex; MTG = middle
 296 temporal gyrus; OP = parietal operculum; PoCG = postcentral gyrus; PrCG = precentral gyrus; preSMA = pre-
 297 supplementary motor area; pSTG = posterior superior temporal gyrus; Put = putamen; rCC = rostral cingulate
 298 zone; SMA = supplementary motor area; SMG = supramarginal gyrus; STN = subthalamic nucleus; Th =
 299 thalamus; vMC = ventral primary motor cortex; vPrCG = ventral precentral gyrus; vSC = ventral primary
 300 somatosensory cortex.

301

302 **Table 2 Brain hubs of speech-related sensorimotor integration**

Brain hub – anatomical label	ROI Label	X	Y	Z
Inferior frontal gyrus, pars opercularis	L IFG	-56	8	8
	R IFG	48	10	2
Pre-supplementary motor area	R preSMA	2	6	60
Ventral primary motor cortex	L vMC	-48	-10	42
	R vMC	54	-8	44
Laryngeal motor cortex [†]	L LMC	-47	-10	34
	R LMC	49	-8	35
Ventral primary somatosensory cortex	L vSC	-56	-12	44
	R vSC	50	-14	34
Parietal operculum, secondary somatosensory cortex	L OP	-60	-12	20
	R OP	60	-10	20
Supramarginal gyrus	L SMG	-54	-40	32
	R SMG	56	-32	20
Heschl's gyrus, primary auditory cortex	L HG	-46	-18	6
	R HG	48	-22	8
Posterior superior temporal gyrus	L pSTG	-54	-34	3
	R pSTG	56	-30	2

303 *All coordinates refer to MNI-space. L = left, R = right. Coordinates were derived from a listen and repeat speech*

304 *task (modified after Darainy et al. 2019; Kumar et al., 2016; Simonyan, 2014).*

305

306 *MRI acquisition protocol*

307 MRI data were acquired in a 3 Tesla Siemens Magnetom Tim Trio scanner (Erlangen, Germany) using
308 an eight-channel, phased-array head coil at the University Medical Center Göttingen, Germany.
309 Sagittal T1-weighted structural data were acquired with a 3D turbo fast low angle shot (FLASH)
310 sequence (TR = 2250ms, TE = 3.26ms, TI = 900ms, flip angle = 9°, 256mm FoV, 7/8 Fourier phase
311 encoding) as whole-brain anatomical reference data at a spatial resolution of $1 \times 1 \times 1 \text{ mm}^3$ voxel
312 size (256×256 matrix). For resting-state fMRI a gradient-echo echo-planar imaging (EPI) sequence
313 (TR = 1800ms, TE = 30ms, flip angle = 70°, parallel acquisition factor 2, 192 mm FoV, 33 slices, 194
314 volumes) was used with isotropic voxels at 3 (mm)^3 and a 64×64 acquisition matrix. We acquired
315 two six-minute rs-fMRI time series at T1 and at T2, respectively, while participants fixated on a cross
316 in an open eyes condition. Due to different head sizes, the rs-fMRI data did not fully cover the
317 cerebellum in some participants. Therefore, the cerebellum was excluded in further rs-fMRI analyses.
318 Participants lay in a supine position in the scanner and wore headphones for noise protection and
319 MR-compatible LCD goggles (VisuaStim XGA, Resonance Technology Inc., Northridge, CA, USA).

320

321 *Rs-fMRI data preprocessing*

322 Structural and functional MRI data were preprocessed and analyzed with CONN functional
323 connectivity toolbox version 18b (Whitfield-Gabrieli and Nieto-Castanon, 2012). The toolbox is based
324 on Matlab and Statistical Parametric Mapping (SPM). The standard preprocessing pipeline of CONN
325 was used with functional realignment, functional centering of the image to (0, 0, 0) coordinates,
326 slice-timing correction, structural centering to (0, 0, 0) coordinates, structural segmentation and
327 normalization to MNI space, and spatial smoothing with a smoothing kernel of 8 mm full-width at
328 half-maximum. Motion parameters and signal outliers were detected via the Artifact Rejection
329 Toolbox set to 95th percentile, which allowed for quantifying participant motion in the scanner and
330 identifying outliers based on the mean signal (Goto et al., 2016; Power et al., 2012). Motion
331 parameters, and white matter and cerebral spinal fluid signals were included as confounds and

332 regressed out during denoising before first-level analysis. Data were denoised using a bandpass filter
333 of 0.009 - 0.08 Hz.

334

335 *ROI-to-ROI functional connectivity analyses*

336 We used the CONN toolbox to analyze rs-fMRI data to determine Fisher-transformed correlation
337 coefficients of bivariate ROI-to-ROI correlations with hemodynamic response function weighting for
338 each of the four sets of ROIs (Fig. 1). We then run four global mixed models ANOVAs with Group
339 (PDS+, FC) as the between-subjects factor and Time and ROIs as within-subjects factors to test
340 intervention-induced neuroplasticity. For multiple comparison correction, we set the connection
341 threshold at seed level $p\text{-FDR} < 0.05$ (two-sided) and the seed-level permutation analysis threshold
342 (based on a Network-Based Statistics by intensity approach¹²) at $p\text{-FDR} < 0.05$. Beta values represent
343 average functional connectivity (Fisher-transformed correlation coefficients) and indicate effect sizes.
344 If Group x Time interactions were significant, we extracted beta values and calculated two-sided
345 paired t -tests in CONN to compare connectivity between T2 and T1 separately for each group.
346 Furthermore, we calculated two-sided unpaired t -tests to analyze group differences separately at T1
347 and T2 (Table 3).

348 PDS- were not included in the global ANOVAs because of the age differences. Still, to test whether
349 the condition to continue to stutter for the period of the treatment influenced brain connectivity, we
350 calculated in CONN additional two-sided independent t -tests, comparing the adjusted connectivity
351 change from T1 to T2 (left IFG-to-LMC, left IFG-to-right pSTG) between PDS+ and PDS. Connectivity
352 changes were adjusted for age and SSI total scores at T1. Because education correlated with age, $r =$
353 0.483, $p < 0.001$, education was not regressed out. Post-hoc we calculated two-sided paired t -tests to
354 compare adjusted connectivity between T2 and T1 separately for each group. Furthermore, we
355 calculated two-sided unpaired t -tests to analyze group differences separately at T1 and T2 (Table 4).

356 Finally, Pearson correlations were calculated in MATLAB (R2018b) to test brain-behavior
357 relationships.

358

359 **Data availability statement**

360 The data that support the findings of this study are available from the corresponding author upon
361 reasonable request.

362

363 **Results**

364 *Computer-assisted intensive intervention improved speech fluency and well-being*

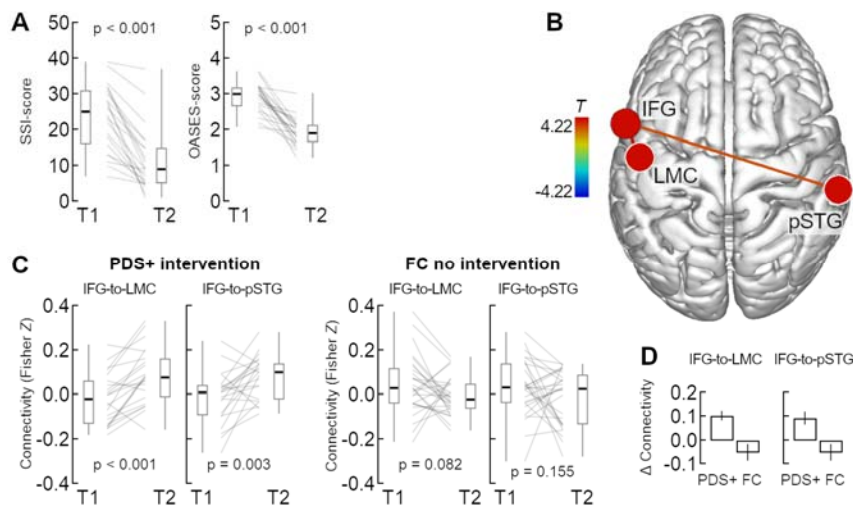
365 The observed reduction in the total scores of the Stuttering Severity Index (SSI-4) and the Overall
366 Assessment of the Speaker's Experience of Stuttering (OASES) indicates a positive effect of stuttering
367 intervention. The robust ANOVA for stuttering severity revealed a significant interaction of Group by
368 Time, $Q = 24.44$, $p < 0.001$, an effect of Group $Q = 48.38$, $p < 0.001$, and an effect of Time $Q = 50.99$, p
369 < 0.001 . Post hoc tests showed that stuttering severity decreased from T1 to T2, $V = 253$, $p < 0.001$, r
370 $= -0.87$ (Fig. 2C) in the intervention group. In the non-intervention groups, on the other hand, the SSI-
371 4 scores remained unchanged with $V = 63$, $p = 0.81$, $r = -0.06$ for PDS- and $V = 58.5$, $p = 0.38$, $r = -0.17$
372 for FC. Similarly, the robust ANOVA for the speaker's experience of stuttering revealed a significant
373 interaction of Group by Time, $Q = 66.73$, $p < 0.001$, an effect of Group $Q = 20.39$, $p < 0.001$ and an
374 effect of time $Q = 74.17$, $p < 0.001$. Post hoc tests revealed a decrease in the OASES-scores between
375 T1 and T2 only in PDS+, $V = 253$, $p < 0.001$, $r = -0.87$ (Fig. 2B). PDS- experienced no changes in their
376 experience with stuttering, $V = 110.5$, $p = 0.29$, $r = -0.25$. Behavioral outcome measures are
377 summarized in Supplementary Table 6.

378

379 *Intervention strengthened sensorimotor network connections*

380 Only one of the four global mixed model ANOVAs revealed significant results. When the
 381 sensorimotor integration network seeds were entered in the analysis, there was no effect of Group
 382 and no effect of Time, but the left IFG showed a Group \times Time \times Target interaction with $F(10, 39) =$
 383 3.46, Intensity = 7.34, $p = 0.021$. Specifically, the interaction was significant for the left IFG-to-left
 384 LMC connection with $\beta = 0.12$, $T(48) = 4.22$, $p = 0.002$, and for the left IFG-to-right pSTG
 385 connection, $\beta = 0.13$, $T(48) = 3.12$, $p = 0.025$ (Fig. 2A). Post-hoc tests showed that connectivity
 386 increased in PDS+ but not in FC, and that pre-treatment connectivity was similar between PDS+ and
 387 FC, but post-treatment connectivity was greater in PDS+ than FC (Table 3).

388



389

390 **Figure 2 Intervention reduced stuttering and strengthened connectivity.** (A) Boxplots display PDS+'s stuttering
 391 severity scores pre- (T1) and post-intervention (T2). (B) Rendered brain surface with connections of the Group \times
 392 Time interaction in the sensorimotor network. (C) Boxplots display rs-fMRI connectivity of PDS+ and fluent
 393 controls (FC) at T1 and T2. (D) Barplots display grand mean connectivity changes, i.e. the Fisher Z difference
 394 between T2 and T1 (\pm SEM). IFG = inferior frontal gyrus; LMC = laryngeal motor cortex; pSTG = posterior
 395 superior temporal gyrus. Boxplots show whiskers from minimum to maximum, interquartile range, and median
 396 values.

397

398 **Table 3 Disentangling the Group \times Time interaction with PDS+ and FC**

Seed - target region	Time				Group		
	T2 > T1	Beta	T (DF)	p	FC vs PDS+	T (DF)	p
left IFG – left LMC	PDS+	0.1	4.91 [#] (21)	< 0.001	T1	1.84 (47.7)	0.072
	FC	-0.051	-1.81 [#] (27)	0.082	T2	-2.8 (35.9)	0.007
left IFG – right pSTG	PDS+	0.094	3.32 [#] (21)	0.003	T1	1.38 (46.7)	0.174
	FC	-0.051	-1.46 [#] (27)	0.155	T2	-3.09 (48.0)	0.003

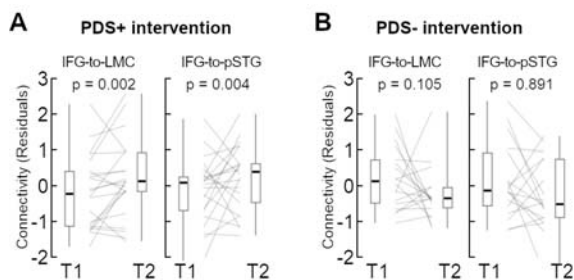
399 [#]Positive values indicate increased connectivity, and negative values indicate decreased connectivity at T2.

400

401 *Connectivity changes relate to fluent speaking*

402 To control whether neuroplasticity was related to the intervention and not to stuttering as a
 403 condition itself, we tested whether significant changes were only evident in PWS+ or whether a
 404 stuttering control group, PDS-, showed similar changes. Because PDS+ and PDS- differed in pre-
 405 intervention stuttering severity and age, we fed SSI-4 total scores and age as variables of no interest
 406 in the model. The Group × Time interaction was significant for the left IFG-to-LMC connection with
 407 beta = 0.17, $T(34) = 3.42$, $p = 0.002$, but not for the left IFG-to-right STG connection with beta = 0.11,
 408 $T(34) = 1.68$, $p = 0.102$. PDS+, but not PDS- showed connectivity increases for both connections
 409 (Table 4). Pre- and post-treatment group comparisons were not significant (Table 4).

410



411

412 **Figure 3 RS-fMRI connectivity corrected for age and stuttering severity (SSI-scores at T1).** Boxplots display
 413 residuals of (A) PDS+ and (B) PDS- at T1 and T2. Boxplots show whiskers from minimum to maximum,

414 *interquartile range, and median values. IFG = inferior frontal gyrus; LMC = laryngeal motor cortex; pSTG =*
 415 *posterior superior temporal gyrus.*

416

417 **Table 4 Disentangling the Group × Time interaction with PDS+ and PDS-**

Seed - target region	Time	Beta	T (DF)	p	Group	T (DF)	p
	T2 > T1				PDS+ vs. PDS-		
¹ left IFG – left LMC	PDS+	0.09	3.64 [#] (19)	0.002	T1	-1.34 (37.9)	0.188
	PDS-	-0.08	-1.73 [#] (15)	0.105	T2	1.45 (36.9)	0.155
¹ left IFG – right pSTG	PDS+	0.11	3.26 [#] (19)	0.004	T1	-0.78 (34.2)	0.442
	PDS-	0.008	0.14 [#] (15)	0.891	T2	1.69 (35.0)	0.100

418 [#]Positive values indicate increased connectivity, and negative values indicate decreased connectivity at T2.

419

420 *No correlation between connectivity changes and fluency enhancement*

421 Neither the change in speech fluency (SSI-4, total score) nor the reappraisal of stuttering (OASES,
 422 total score) correlated with the changes in rs-connectivity of PDS+, all $p > 0.05$.

423

424 Discussion

425 A one-year, biofeedback-based, speech restructuring training program sustainably facilitated speech
 426 fluency of patients with developmental stuttering. Furthermore, neural reorganization included a
 427 strengthened synchronization of the IFG pars opercularis with the left LMC and the right pSTG. Thus,
 428 resting-state fMRI showed that intensive stuttering intervention remodeled the command-to-
 429 execution pathway and the sensory-to-motor pathway within the sensorimotor integration network.
 430 Hence, we show here for the first time that a computer-assisted, biofeedback-based, intensive

431 speech training program induced functionally specific, long-term focal changes in task-free brain
432 connectivity.

433

434 *Therapy induced a positive shift of brain connectivity*

435 We measured, task-free BOLD fMRI fluctuations with ROI-to-ROI connectivity matrices. Chosen
436 metrics characterize connectivity between pairs of ROIs among predefined sets of regions and yield
437 values varying above and below zero. The metrics called ‘connectivity’ is, at its core, a \tanh^{-1} -
438 transformed *correlation coefficient*. The naming ‘connectivity’ can be counter-intuitive when a
439 measure with negative values is concerned. We stuck to this nomenclature, following (Biswal et al.,
440 1995; Whitfield-Gabrieli and Nieto-Castanon, 2012). How then can we interpret negative values and
441 changes? The activity waveforms at the two sites of interest underly a number of influences. Some
442 might be direct, between the regions, others indirect. The sum of all influences create the observed
443 correlation, reported as ‘connectivity’. Negative connectivity values signify a negative correlation
444 between the signal waveforms of the two brain regions of interest. This connectivity reflects, in a
445 single number, the net effects of those multiple influences, some driving positive correlations, some
446 driving negative correlations. The overall group median around 0 is consistent with the idea that
447 positively correlating influences and negatively correlating influences are balanced. The fluctuations
448 observed for individual participants, the change of sign from T1 to T2, indicates that the relative
449 magnitude of positive and negatively correlating influences varies. In this framework, the therapy-
450 related shift towards more positive connectivity has to be interpreted as an increase of the
451 influences that drive positive correlations between the two sites. In some participants, this effect
452 occurs relative to a baseline of an overall negative correlation, leading to less negative ‘connectivity’.
453 This shift towards more positively correlating influences on the sensorimotor areas, follows the
454 training and usage of reshaped speech patterns. This is consistent with the hypothesis that the
455 sensorimotor integration necessary for this re(learning) is the cause of this more positively
456 correlating influence.

457

458 *Stuttering intervention strengthens connectivity of the left IFG with the left laryngeal motor cortex*

459 The studied intervention encompassed one year of learning and practicing a new speech technique.

460 This speech technique comprises soft voice onsets, consonant lenitions, and controlled sound

461 prolongations (Euler et al., 2009). Thus, voicing and timing are the key features under change

462 throughout the acquisition of the new speech technique. The control of voicing is based on the

463 neural control of the larynx and involves the LMC (Bouchard et al., 2013; Brown et al., 2008; Olthoff

464 et al., 2008; Rödel et al., 2004; Simonyan, 2014; Simonyan et al., 2009), while the control of speech

465 timing involves activity of the posterior part of the inferior frontal gyrus pars opercularis (Clos et al.,

466 2013; Long et al., 2016; Neef et al., 2016). Accordingly, the intensive training incorporated two brain

467 regions, the left LMC and the left IFG, that provide essential neural contributions to fluent speech

468 production.

469 We found that the intervention strengthened connectivity between the left IFG and the left LMC in

470 the current study. This finding is also consistent with the involvement of the left posterior IFG and

471 left motor cortex in motor learning in general (Papitto et al., 2019) and with the particular

472 involvement of the posterior IFG and the left LMC in speech motor learning (Darainy et al., 2019;

473 Rauschecker et al., 2008). The IFG and the orofacial motor cortex share direct connections (Greenlee

474 et al., 2004) and are commonly co-active under task- and resting-state conditions (Simonyan et al.,

475 2009; Simonyan and Fuertinger, 2015). Furthermore, theories on speech motor control assume the

476 posterior region of the IFG to link the target speech unit to an articulatory code that is subsequently

477 implemented by the motor cortices, which finally orchestrate the articulators, including the larynx

478 (Guenther, 2016). Hence, vital functional connectivity between the left IFG and left LMC is essential

479 for acquiring a new speech technique.

480

481 *Stuttering intervention strengthens connectivity of the left IFG with the right posterior superior*
482 *temporal gyrus*

483 The intervention strengthened co-activity between the left IFG and the right pSTG. The speech motor
484 system has to monitor the auditory feedback signal to correct articulatory errors in natural speech
485 rapidly. Speech-related auditory feedback control involves the right pSTG and task-related co-
486 activations of the left posterior IFG with bilateral pSTGs (Behroozmand et al., 2015; Guenther, 2016;
487 Guenther et al., 2006; Niziolek and Guenther, 2013; Tourville et al., 2008). The DIVA (directions into
488 velocities of articulators) model of speech motor control suggests that the posterior IFG provides
489 feedforward control signals, and the pSTG conveys feedback-based corrective signals (Guenther,
490 2016). In addition, the right pSTG is associated with spectral auditory feedback control, whereas the
491 left pSTG is more involved during changes in the temporal domain of auditory feedback (Floegel et
492 al., 2020). Learning and practicing a new speech technique addresses neural circuitries of auditory
493 feedback monitoring because patients are constantly required to adjust their speech to fit the new
494 sound pattern of fluency shaping. We suggest that the increased co-activity between left IFG and
495 right pSTG could reflect the frequent recruitment of both brain regions and auditory spectral
496 feedback control mechanisms during learning and practicing the new speech pattern.

497 Interestingly in our study, PDS+ had no increase of left-hemispheric functional connectivity between
498 the ventral motor cortex vMC and pSTG, contrary to observations in a former study (Kell et al., 2018).
499 This former study used task-related fMRI and showed a reduced left pSTS-to-vMC connectivity before
500 therapy and a strengthened left aSTG-to-vMC connectivity after therapy in PDS+. One possible
501 explanation of why we could not find such an intervention-associated strengthening of left auditory-
502 to-motor coupling could be the seeds' locations in the current study. While the IFG seeds overlap,
503 MC and STG ROIs are not overlapping. However, another difference between both studies is the time
504 between T1 and T2. The current study investigated the long-term effects. Thus, strengthened
505 connectivity, including the left pSTG could be missing as participants might have shifted auditory
506 feedback control strategies throughout the intervention. One could speculate that temporal features

507 related to the soft production of consonants might be more critical at the early stage of speech
508 motor learning, while spectral features such as vowel length and prosody come later into play.

509

510 *Resting-state connectivity is improbable to reflect compensatory brain activity*

511 Here, we measured MRI signal fluctuations in the absence of response demands or external
512 stimulation to describe intervention-induced changes in the speech function-related sensorimotor
513 integration network. It is assumed that spontaneous brain activity at rest relates to the underlying
514 anatomical circuitry (Deco et al., 2013) as supported by diffusion-weighted imaging (Hagmann et al.,
515 2008; Honey et al., 2009). Specifically, it has been suggested that spatially and temporally correlated
516 brain activity at rest arises from neuronal noise between brain areas that share anatomical
517 connections (Deco et al., 2013). In this respect, the current study extends the scope of previous
518 studies where task-related changes in brain activity were observed as a result of the very same
519 intensive stuttering intervention (Kell et al., 2018, 2009; Neumann et al., 2005, 2003). Nevertheless,
520 the current finding of increased sensorimotor learning does not contradict previous conclusions, i.e.,
521 normalization of brain activity after intervention (Kell et al., 2018, 2009; Neumann et al., 2005, 2003)
522 as findings are not directly comparable. First, whereas this study investigates long-term effects, the
523 former study tested short-term brain changes directly after the on-site intervention. In addition, the
524 analyses methods of this study highlight learning-related changes and cannot represent neuronal
525 processes related to the occurrence of speech disfluencies. On the other hand, task-related
526 neuroimaging results from learning studies might be confounded by behavioral changes. Using
527 resting-state activity as a neural marker of neuroplasticity rules out that changes in brain activity
528 were induced by changes in task performance (Darainy et al., 2019). In fact, here we provided a
529 purely neurophysiological index of neuroplasticity in the context of an intensive stuttering
530 intervention.

531

532 *No correlations between behavioral and connectivity changes*

533 Consistent with our findings, some previous studies reported no correlations between changes in
534 brain activity and changes in speech fluency (Neumann et al., 2003; Toyomura et al., 2015). Others
535 observed correlations between post-treatment speech fluency and task-based brain activity and
536 connectivity (Kell et al., 2018, 2009; Lu et al., 2017) or task-free resting-state connectivity (Lu et al.,
537 2012). These previously reported resting-state functional connectivity changes involved the
538 cerebellum and related the left declive and vermis area to intervention-induced speech fluency (Kell
539 et al., 2009; Lu et al., 2012; Toyomura et al., 2015). In our study, the field of view did not cover the
540 cerebellum, and thus cerebellar ROIs were not included in the analyses. For this reason, it was not
541 possible to test intervention-induced reorganization of the cerebellum.

542 However, the question still remains of why the significant changes in connectivity reported here do
543 not correlate with speech fluency changes.

544

545 *Connectivity changes involve brain hubs of the sensorimotor integration network*

546 We observed no connectivity changes between brain hubs subserving speech planning processes and
547 articulatory convergence. Speech planning processes address working memory resources, and
548 related brain activity is shaped by sequencing demands, syllable complexity, and length (Bohland and
549 Guenther, 2006; Rottschy et al., 2012; Segawa et al., 2015). Articulatory convergence relates to the
550 joint coordination of articulatory movements across the multiple articulatory subsystems (Guenther,
551 2016). During the intervention, the main focus of practice was controlling the larynx to use soft voice
552 onsets and consonants together with slow speech. This technique requires primarily sensorimotor
553 control and monitoring of the intended auditory target and might unburden or even facilitate speech
554 planning and articulatory convergence. Thus, speech planning processes or the coordination of
555 articulators were not addressed to result in task-free functional connectivity changes. Our
556 observation is in line with a recent neuroimaging study showing that PDS exhibit no deficit in learning

557 to produce novel phoneme sequences (Masapollo et al., 2021); task-related fMRI data showed no
558 difference in brain activity between PDS and controls for the articulation of practiced and novel
559 pseudowords. Thus, sensorimotor learning and feedback processing in the context of voice control
560 may be the main drivers of the neuroplasticity in the current study.

561 Previous studies also related intervention-associated functional activity and connectivity changes to
562 sensorimotor integration (Kell et al., 2018) and normalized prosody processing (Kell et al., 2018).
563 They suggested that fluency-inducing techniques synchronize a disturbed signal transmission
564 between auditory, speech motor planning, and motor areas (Neumann et al., 2003). Moreover, the
565 main conclusion from these previous task-fMRI studies is that fluency-shaping training normalizes
566 brain activity. This conclusion is based on the observation that pretreatment activity was reduced in
567 the left IFG and increased in the right IFG, but normalized to a level that is comparable to the activity
568 in controls after the intervention (Kell et al., 2018, 2009; Neumann et al., 2003). However, in the
569 present study, pretreatment rs-fMRI connectivity was similar between PDS+ and FC. There was
570 neither altered resting-state connectivity of the left nor of the right IFG. Only post-treatment
571 connectivity was increased between hubs within the set of sensorimotor integration ROIs. Thus, the
572 current findings do not directly support the previous normalization account. Instead, current rs-fMRI
573 data suggest that fluency-shaping training recruits connections that support sensorimotor learning
574 and integration. One could speculate that people who do not stutter would recruit similar
575 connections to learn a new speaking behavior and that intensive therapy addresses a vital brain
576 function. This interpretation is in line with rs-fMRI connectivity changes observed after short-term
577 speech motor adaptation (Darainy 2019).

578 The increased task-fMRI activity of the right IFG is a signature of persistent developmental stuttering
579 (Belyk et al., 2015; Brown et al., 2005; Budde et al., 2014; Neef et al., 2015). On the one hand,
580 previous studies associate the therapy-associated reduction of this hyperactivity in the right IFG with
581 compensatory mechanisms (Kell et al., 2009; Neumann et al., 2003; Preibisch et al., 2003). On the
582 other hand, previous studies from our group suggest that this hyperactivity might be related to

583 hyperactive action inhibition, which could indicate a pathophysiological mechanism that causes
584 stuttering (Hartwigsen et al., 2019; Neef et al., 2018, 2016). Here we show, that the connectivity
585 between the set of ROIs forming the inhibition network remained unchanged. This observation also
586 supports the view that fluency-shaping training addresses vital sensorimotor learning and integration
587 structures rather than the pathophysiological structures themselves.

588

589 *Perspectives concerning other therapeutic approaches to ameliorate stuttering*

590 Common stuttering interventions consist of (1) speech motor interventions partly modifying or
591 entirely reshaping laryngeal, articulatory, or respiratory movements, (2) feedback and technology
592 interventions which use, e.g., delayed auditory feedback to enhance fluency, or visual feedback to
593 support speech motor interventions, (3) behavioral modification interventions, or (4) cognitive
594 interventions improving psychological well-being, self-confidence, and self-conception. The current
595 and previous studies tested neurofunctional correlates of brain reorganization for the first two
596 approaches. However, the neurobiological foundation of an intervention-induced relief from
597 stuttering induced by the other two approaches, such as, for example, the cognitive-behavior
598 intervention (Menzies et al., 2016), would be worth studying.

599 Of most significant importance are future studies in children with persistent stuttering. Cross-
600 sectional morphological studies with children who stutter imply a primary deficit in left frontal brain
601 hubs of speech motor control (Beal et al., 2013; Chang et al., 2019; Garnett et al., 2018; Koenraads et
602 al., 2020). Moreover, compared to fluent peers, children who stutter exhibited a reduced activation
603 of the left dorsal IFG and the left premotor cortex during overt speech production, as shown by fNIRS
604 (Walsh et al., 2017). However, in particular, rs-fMRI is a feasible approach to extend our knowledge
605 about neuroplasticity related to improved fluency or even recovery in young children because it is
606 not required to engage them in a speech task. A longitudinal rs-fMRI study revealed aberrant
607 network organizations in children who persist in stuttering and in children who recovered from

608 stuttering (Chang et al., 2018). Therefore, a significant future objective is to disentangle intervention-
609 associated neural reorganization and maladaptive changes related to manifestation. A better
610 understanding of conditions that facilitate neurotypical brain functioning in children who stutter
611 could provide the neurobiological foundation of therapeutic strategies that sustainably enhance
612 fluency.

613

614 *Limitations*

615 The current study was a non-interventional prospective study. Unlike a clinical trial, data collection
616 and patient participation did not interfere with the choice of treatment, sample collection,
617 procedures, or the treatment itself. Specifically, we collected MRI data without interfering with
618 timing or choice of treatment. It is essential to acknowledge that, like everyone else, persons with
619 stuttering try to get the best out of life, and participating in on-site intensive training for multiple
620 weeks means being away from work, family, and daily obligations. For this reason, the chosen design
621 helped us recruit as many participants as possible. However, this approach resulted in the problem
622 that while PDS+ and FC were comparable for age, PDS+ and PDS- differed for age and stuttering
623 severity. Strikingly, our statistics yielded results that were neither influenced by age nor by stuttering
624 severity at T1. Nevertheless, to enhance comparability between groups of stuttering participants,
625 future studies should match participants according to their stuttering severity.

626 In addition, the study protocol included a task-related fMRI of covert speaking (not reported here),
627 which was acquired before resting-state. Intervention-related changes in brain activity were evident
628 in the left and right rolandic operculum, the right IFG pars triangularis, the right SMG, the left STG,
629 the left temporal pole, and the left amygdala (Primaßin, 2019). However, none of these regions
630 showed intervention related-changes in task-free resting-state activity. Furthermore, the MRI
631 protocol was kept the same for all participants, and thus, possible carry-over effects would have

632 affected all groups in a similar way. Accordingly, although we cannot entirely exclude carry-over
633 effects, these two aspects make them less likely.

634 Last, test-retest reliability of metrics of spontaneous BOLD-fMRI fluctuations seems to strongly vary
635 between networks (Noble et al., 2019), regions (Donnelly-Kehoe et al., 2019), and over pairs of
636 regions (Pannunzi et al., 2017). For example, the default mode network and frontal network seem
637 most reliable, and subcortical networks seem least reliable (Noble et al., 2019), which might be
638 related to stronger connectivity estimates in cortical compared to subcortical networks (Noble et al.,
639 2017). Selected sets of seed ROIs were defined based on task-fMRI activity, an accepted approach to
640 evaluate rs-fMRI activity (Hausman et al., 2020; Pando-Naude et al., 2019). This approach was
641 motivated by the presumption that in the absence of a task, brain regions that typically activate
642 together during task performance show strong correlations with one another at rest (Deco et al.,
643 2013, 2011; Vahdat et al., 2011), and the current study was particularly interested in the brain hubs
644 involved in speech motor learning and processing. Because the selected sets of ROIs do not
645 constitute classical resting-state fMRI networks, such as the default network, they seem particularly
646 susceptible to variability and thus to a low test-retest reliability. Reliability across sessions is vital for
647 interpreting longitudinal studies (Birn et al., 2013). The statistical significance of increased
648 connectivity in the face of such variability suggests to us that the effect is of considerable magnitude.

649

650 **Conclusion**

651 A one-year practice of fluency-shaping speech techniques boosts the synchrony of spontaneous brain
652 activity in core hubs of speech timing and voice control. Thus, successful speech restructuring shapes
653 sensorimotor integration networks and is reflected in a long-lasting, focal, neurofunctional
654 reorganization.

655

656 **References**

- 657 Albert, N.B., Robertson, E.M., Miall, C.R., 2009. The resting human brain and motor learning. *Current*
658 *Biology* 19, 1023–1027. <https://doi.org/10.1016/j.cub.2009.04.028>
- 659 Andreatta, R.D., Stemple, J.C., Joshi, A., Jiang, Y., 2010. Task-related differences in temporo-parietal
660 cortical activation during human phonatory behaviors. *Neuroscience Letters* 484, 51–55.
661 <https://doi.org/10.1016/j.neulet.2010.08.017>
- 662 Aron, Poldrack, 2006. Cortical and subcortical contributions to Stop signal response inhibition: role of
663 the subthalamic nucleus. *J Neurosci* 26, 2424–2433.
664 <https://doi.org/10.1523/JNEUROSCI.4682-05.2006>
- 665 Beal, D.S., Gracco, V.L., Brettschneider, J., Kroll, R.M., De Nil, L.F., 2013. A voxel-based morphometry
666 (VBM) analysis of regional grey and white matter volume abnormalities within the speech
667 production network of children who stutter. *Cortex* 49, 2151–2161.
668 <https://doi.org/10.1016/j.cortex.2012.08.013>
- 669 Behroozmand, R., Shebek, R., Hansen, D.R., Oya, H., Robin, D.A., Howard, M.A., Greenlee, J.D.W.,
670 2015. Sensory-motor networks involved in speech production and motor control: an fMRI
671 study. *Neuroimage* 109, 418–428. <https://doi.org/10.1016/j.neuroimage.2015.01.040>
- 672 Belyk, M., Kraft, S.J., Brown, S., 2015. Stuttering as a trait or state - an ALE meta-analysis of
673 neuroimaging studies. *Eur. J. Neurosci.* 41, 275–284. <https://doi.org/10.1111/ejn.12765>
- 674 Birn, R.M., Molloy, E.K., Patriat, R., Parker, T., Meier, T.B., Kirk, G.R., Nair, V.A., Meyerand, M.E.,
675 Prabhakaran, V., 2013. The effect of scan length on the reliability of resting-state fMRI
676 connectivity estimates. *Neuroimage* 83, 550–558.
677 <https://doi.org/10.1016/j.neuroimage.2013.05.099>
- 678 Biswal, B., Yetkin, F.Z., Haughton, V.M., Hyde, J.S., 1995. Functional connectivity in the motor cortex
679 of resting human brain using echo-planar mri. *Magnetic Resonance in Medicine* 34, 537–541.
680 <https://doi.org/10.1002/mrm.1910340409>
- 681 Bohland, J.W., Guenther, F.H., 2006. An fMRI investigation of syllable sequence production.
682 *Neuroimage* 32, 821–841. <https://doi.org/10.1016/j.neuroimage.2006.04.173>
- 683 Bouchard, K.E., Mesgarani, N., Johnson, K., Chang, E.F., 2013. Functional organization of human
684 sensorimotor cortex for speech articulation. *Nature* 495, 327–332.
685 <https://doi.org/10.1038/nature11911>
- 686 Brown, S., Ingham, R.J., Ingham, J.C., Laird, A.R., Fox, P.T., 2005. Stuttered and fluent speech
687 production: an ALE meta-analysis of functional neuroimaging studies. *Hum Brain Mapp* 25,
688 105–117. <https://doi.org/10.1002/hbm.20140>
- 689 Brown, S., Ngan, E., Liotti, M., 2008. A Larynx Area in the Human Motor Cortex. *Cereb Cortex* 18,
690 837–845. <https://doi.org/10.1093/cercor/bhm131>
- 691 Budde, K., Barron, D.S., Fox, P.T., 2014. Stuttering, induced fluency, and natural fluency: A
692 hierarchical series of activation likelihood estimation meta-analyses. *Brain and Language* 99–
693 107.
- 694 Calmels, C., 2020. Neural correlates of motor expertise: Extensive motor training and cortical
695 changes. *Brain Res.* 1739, 146323. <https://doi.org/10.1016/j.brainres.2019.146323>
- 696 Chang, S.-E., Angstadt, M., Chow, H.M., Etchell, A.C., Garnett, E.O., Choo, A.L., Kessler, D., Welsh,
697 R.C., Sripada, C., 2018. Anomalous network architecture of the resting brain in children who
698 stutter. *Journal of Fluency Disorders* 55, 46–67. <https://doi.org/10.1016/j.jfludis.2017.01.002>
- 699 Chang, S.-E., Garnett, E.O., Etchell, A., Chow, H.M., 2019. Functional and Neuroanatomical Bases of
700 Developmental Stuttering: Current Insights. *Neuroscientist* 25, 566–582.
701 <https://doi.org/10.1177/1073858418803594>
- 702 Clos, M., Amunts, K., Laird, A.R., Fox, P.T., Eickhoff, S.B., 2013. Tackling the multifunctional nature of
703 Broca's region meta-analytically: Co-activation-based parcellation of area 44. *Neuroimage*
704 83, 174–188. <https://doi.org/10.1016/j.neuroimage.2013.06.041>
- 705 Darainy, M., Vahdat, S., Ostry, D.J., 2019. Neural Basis of Sensorimotor Plasticity in Speech Motor
706 Adaptation. *Cerebral Cortex* 29, 2876–2889. <https://doi.org/10.1093/cercor/bhy153>
- 707 De Nil, L.F., Beal, D.S., Lafaille, S.J., Kroll, R.M., Crawley, A.P., Gracco, V.L., 2008. The effects of
708 simulated stuttering and prolonged speech on the neural activation patterns of stuttering

- 709 and nonstuttering adults. *Brain Lang* 107, 114–123.
710 <https://doi.org/10.1016/j.bandl.2008.07.003>
- 711 De Nil, L.F., Kröll, R.M., Houle, S., 2001. Functional neuroimaging of cerebellar activation during single
712 word reading and verb generation in stuttering and nonstuttering adults. *Neurosci Lett* 302,
713 77–80. [https://doi.org/10.1016/s0304-3940\(01\)01671-8](https://doi.org/10.1016/s0304-3940(01)01671-8)
- 714 De Nil, L.F., Kröll, R.M., Lafaille, S.J., Houle, S., 2003. A positron emission tomography study of short-
715 and long-term treatment effects on functional brain activation in adults who stutter. *J*
716 *Fluency Disord* 28, 357–379; quiz 379–380. <https://doi.org/10.1016/j.jfludis.2003.07.002>
- 717 Deco, G., Jirsa, V.K., McIntosh, A.R., 2011. Emerging concepts for the dynamical organization of
718 resting-state activity in the brain. *Nat Rev Neurosci* 12, 43–56.
719 <https://doi.org/10.1038/nrn2961>
- 720 Deco, G., Ponce-Alvarez, A., Mantini, D., Romani, G.L., Hagmann, P., Corbetta, M., 2013. Resting-State
721 Functional Connectivity Emerges from Structurally and Dynamically Shaped Slow Linear
722 Fluctuations. *J. Neurosci.* 33, 11239–11252. [https://doi.org/10.1523/JNEUROSCI.1091-](https://doi.org/10.1523/JNEUROSCI.1091-13.2013)
723 13.2013
- 724 Donnelly-Kehoe, P., Saenger, V.M., Lisofsky, N., Kühn, S., Kringelbach, M.L., Schwarzbach, J.,
725 Lindenberger, U., Deco, G., 2019. Reliable local dynamics in the brain across sessions are
726 revealed by whole-brain modeling of resting state activity. *Hum Brain Mapp* 40, 2967–2980.
727 <https://doi.org/10.1002/hbm.24572>
- 728 Euler, H.A., Gudenberg, A.W. v, Jung, K., Neumann, K., 2009. Computergestützte Therapie bei
729 Redeflussstörungen: Die langfristige Wirksamkeit der Kasseler Stottertherapie (KST). *Sprache*
730 *· Stimme · Gehör* 33, 193–202. <https://doi.org/10.1055/s-0029-1242747>
- 731 Euler, H.A., Merkel, A., Hente, K., Neef, N., Wolff von Gudenberg, A., Neumann, K., 2021. Speech
732 restructuring group treatment for 6-to-9-year-old children who stutter: A therapeutic trial. *J*
733 *Commun Disord* 89, 106073. <https://doi.org/10.1016/j.jcomdis.2020.106073>
- 734 Floegel, M., Fuchs, S., Kell, C.A., 2020. Differential contributions of the two cerebral hemispheres to
735 temporal and spectral speech feedback control. *Nat Commun* 11, 2839.
736 <https://doi.org/10.1038/s41467-020-16743-2>
- 737 Fox, M.D., Corbetta, M., Snyder, A.Z., Vincent, J.L., Raichle, M.E., 2006. Spontaneous neuronal activity
738 distinguishes human dorsal and ventral attention systems. *PNAS* 103, 10046–10051.
739 <https://doi.org/10.1073/pnas.0604187103>
- 740 Garnett, E.O., Chow, H.M., Nieto-Castañón, A., Tourville, J.A., Guenther, F.H., Chang, S.-E., 2018.
741 Anomalous morphology in left hemisphere motor and premotor cortex of children who
742 stutter. *Brain* 141, 2670–2684. <https://doi.org/10.1093/brain/awy199>
- 743 Ghahremani, A., Wessel, J.R., Udupa, K., Neagu, B., Zhuang, P., Saha, U., Kalia, S.K., Hodaie, M.,
744 Lozano, A.M., Aron, A.R., Chen, R., 2018. Stopping and slowing manual and spoken
745 responses: Similar oscillatory signatures recorded from the subthalamic nucleus. *Brain Lang*
746 176, 1–10. <https://doi.org/10.1016/j.bandl.2017.10.009>
- 747 Goto, M., Abe, O., Miyati, T., Yamasue, H., Gomi, T., Takeda, T., 2016. Head Motion and Correction
748 Methods in Resting-state Functional MRI. *Magn Reson Med Sci* 15, 178–186.
749 <https://doi.org/10.2463/mrms.rev.2015-0060>
- 750 Greenlee, J.D.W., Oya, H., Kawasaki, H., Volkov, I.O., Kaufman, O.P., Kovach, C., Howard, M.A.,
751 Brugge, J.F., 2004. A Functional Connection Between Inferior Frontal Gyrus and Orofacial
752 Motor Cortex in Human. *Journal of Neurophysiology* 92, 1153–1164.
753 <https://doi.org/10.1152/jn.00609.2003>
- 754 Guenther, F.H., 2016. *Neural Control of Speech*. MIT Press, Cambridge, Mass.
- 755 Guenther, F.H., Ghosh, S.S., Tourville, J.A., 2006. Neural modeling and imaging of the cortical
756 interactions underlying syllable production. *Brain Lang* 96, 280–301.
757 <https://doi.org/10.1016/j.bandl.2005.06.001>
- 758 Hagmann, P., Cammoun, L., Gigandet, X., Meuli, R., Honey, C.J., Wedeen, V.J., Sporns, O., 2008.
759 Mapping the Structural Core of Human Cerebral Cortex. *PLOS Biology* 6, e159.
760 <https://doi.org/10.1371/journal.pbio.0060159>

- 761 Hartwigsen, G., Neef, N.E., Camilleri, J.A., Margulies, D.S., Eickhoff, S.B., 2019. Functional Segregation
762 of the Right Inferior Frontal Gyrus: Evidence From Coactivation-Based Parcellation. *Cereb.*
763 *Cortex* 29, 1532–1546. <https://doi.org/10.1093/cercor/bhy049>
- 764 Hausman, H.K., Jackson, T.B., Goen, J.R.M., Bernard, J.A., 2020. From Synchrony to Asynchrony:
765 Cerebellar-Basal Ganglia Functional Circuits in Young and Older Adults. *Cereb Cortex* 30, 718–
766 729. <https://doi.org/10.1093/cercor/bhz121>
- 767 Hayes, A.F., Krippendorff, K., 2017. Answering the call for a standard reliability measure for coding
768 data. *Communication Methods and Measures* 1, 77–89.
- 769 Hickok, Houde, J., Rong, F., 2011. Sensorimotor Integration in Speech Processing: Computational
770 Basis and Neural Organization. *Neuron* 69, 407–422.
771 <https://doi.org/10.1016/j.neuron.2011.01.019>
- 772 Honey, C.J., Sporns, O., Cammoun, L., Gigandet, X., Thiran, J.P., Meuli, R., Hagmann, P., 2009.
773 Predicting human resting-state functional connectivity from structural connectivity. *PNAS*
774 106, 2035–2040. <https://doi.org/10.1073/pnas.0811168106>
- 775 Ingham, R.J., Ingham, J.C., Euler, H.A., Neumann, K., 2018. Stuttering treatment and brain research in
776 adults: A still unfolding relationship. *J Fluency Disord* 55, 106–119.
777 <https://doi.org/10.1016/j.jfludis.2017.02.003>
- 778 Kell, C.A., 2012. Resting-state MRI: a peek through the keyhole on therapy for stuttering. *Neurology*
779 79, 614–615. <https://doi.org/10.1212/WNL.0b013e31826357fe>
- 780 Kell, C.A., Neumann, K., Behrens, M., Gudenberg, A.W. von, Giraud, A.-L., 2018. Speaking-related
781 changes in cortical functional connectivity associated with assisted and spontaneous
782 recovery from developmental stuttering. *Journal of Fluency Disorders* 55, 135–144.
783 <https://doi.org/10.1016/j.jfludis.2017.02.001>
- 784 Kell, C.A., Neumann, K., von Kriegstein, K., Posenenske, C., Gudenberg, V., W, A., Euler, H., Giraud, A.-
785 L., 2009. How the brain repairs stuttering. *Brain* 132, 2747–2760.
786 <https://doi.org/10.1093/brain/awp185>
- 787 Koenraads, S.P.C., van der Schroeff, M.P., van Ingen, G., Lamballais, S., Tiemeier, H., Baatenburg de
788 Jong, R.J., White, T., Franken, M.C., Muetzel, R.L., 2020. Structural brain differences in pre-
789 adolescents who persist in and recover from stuttering. *Neuroimage Clin* 27, 102334.
790 <https://doi.org/10.1016/j.nicl.2020.102334>
- 791 Kumar, V., Croxson, P.L., Simonyan, K., 2016. Structural Organization of the Laryngeal Motor Cortical
792 Network and Its Implication for Evolution of Speech Production. *The Journal of Neuroscience*
793 36, 4170–4181. <https://doi.org/10.1523/JNEUROSCI.3914-15.2016>
- 794 Long, M.A., Katlowitz, K.A., Svirsky, M.A., Clary, R.C., Byun, T.M., Majaj, N., Oya, H., Howard III, M.A.,
795 Greenlee, J.D.W., 2016. Functional Segregation of Cortical Regions Underlying Speech Timing
796 and Articulation. *Neuron* 89, 1187–1193. <https://doi.org/10.1016/j.neuron.2016.01.032>
- 797 Lu, C., Chen, C., Ning, N., Ding, G., Guo, T., Peng, D., Yang, Y., Li, K., Lin, C., 2010. The neural
798 substrates for atypical planning and execution of word production in stuttering. *Exp Neurol*
799 221, 146–156. <https://doi.org/10.1016/j.expneurol.2009.10.016>
- 800 Lu, C., Chen, C., Peng, D., You, W., Zhang, X., Ding, G., Deng, X., Yan, Q., Howell, P., 2012. Neural
801 anomaly and reorganization in speakers who stutter: a short-term intervention study.
802 *Neurology* 79, 625–632. <https://doi.org/10.1212/WNL.0b013e31826356d2>
- 803 Lu, C., Zheng, L., Long, Y., Yan, Q., Ding, G., Liu, L., Peng, D., Howell, P., 2017. Reorganization of brain
804 function after a short-term behavioral intervention for stuttering. *Brain and Language* 168,
805 12–22. <https://doi.org/10.1016/j.bandl.2017.01.001>
- 806 Margulies, D.S., Kelly, A.M.C., Uddin, L.Q., Biswal, B.B., Castellanos, F.X., Milham, M.P., 2007.
807 Mapping the functional connectivity of anterior cingulate cortex. *Neuroimage* 37, 579–588.
808 <https://doi.org/10.1016/j.neuroimage.2007.05.019>
- 809 Masapollo, M., Segawa, J.A., Beal, D.S., Tourville, J.A., Nieto-Castañón, A., Heyne, M., Frankford, S.A.,
810 Guenther, F.H., 2021. Behavioral and Neural Correlates of Speech Motor Sequence Learning
811 in Stuttering and Neurotypical Speakers: An fMRI Investigation. *Neurobiology of Language* 2,
812 106–137. https://doi.org/10.1162/nol_a_00027

- 813 Max Ludo, Caruso Anthony J., 1997. Contemporary Techniques for Establishing Fluency in the
814 Treatment of Adults Who Stutter. *Contemporary Issues in Communication Science and*
815 *Disorders* 24, 39–46. https://doi.org/10.1044/cicsd_24_S_39
- 816 Menzies, R., O’Brian, S., Lowe, R., Packman, A., Onslow, M., 2016. International Phase II clinical trial
817 of CBTPsych: A standalone Internet social anxiety treatment for adults who stutter. *J Fluency*
818 *Disord* 48, 35–43. <https://doi.org/10.1016/j.jfludis.2016.06.002>
- 819 Neef, N.E., Anwander, A., Bütfering, C., Schmidt-Samoa, C., Friederici, A.D., Paulus, W., Sommer, M.,
820 2018. Structural connectivity of right frontal hyperactive areas scales with stuttering severity.
821 *Brain* 141, 191–204. <https://doi.org/10.1093/brain/awx316>
- 822 Neef, N.E., Anwander, A., Friederici, A.D., 2015. The Neurobiological Grounding of Persistent
823 Stuttering: from Structure to Function. *Curr Neurol Neurosci Rep* 15, 63.
824 <https://doi.org/10.1007/s11910-015-0579-4>
- 825 Neef, N.E., Bütfering, C., Anwander, A., Friederici, A.D., Paulus, W., Sommer, M., 2016. Left posterior-
826 dorsal area 44 couples with parietal areas to promote speech fluency, while right area 44
827 activity promotes the stopping of motor responses. *NeuroImage* 142, 628–644.
828 <https://doi.org/10.1016/j.neuroimage.2016.08.030>
- 829 Neumann, K., Euler, H.A., Gudenberg, A.W. von, Giraud, A.-L., Lanfermann, H., Gall, V., Preibisch, C.,
830 2003. The nature and treatment of stuttering as revealed by fMRI: a within- and between-
831 group comparison. *Journal of Fluency Disorders, Brain Imaging and Stuttering* 28, 381–410.
832 <https://doi.org/10.1016/j.jfludis.2003.07.003>
- 833 Neumann, K., Euler, H.A., Kob, M., Gudenberg, A.W. v, Giraud, A.-L., Weissgerber, T., Kell, C.A., 2018.
834 Assisted and unassisted recession of functional anomalies associated with dysprosody in
835 adults who stutter. *Journal of Fluency Disorders* 55, 120–134.
836 <https://doi.org/10.1016/j.jfludis.2017.09.003> [Titel anhand dieser DOI in Citavi-Projekt
837 übernehmen]
- 838 Neumann, K., Preibisch, C., Euler, H.A., Gudenberg, A.W. von, Lanfermann, H., Gall, V., Giraud, A.-L.,
839 2005. Cortical plasticity associated with stuttering therapy. *Journal of Fluency Disorders* 30,
840 23–39. <https://doi.org/10.1016/j.jfludis.2004.12.002>
- 841 Niziolek, C.A., Guenther, F.H., 2013. Vowel Category Boundaries Enhance Cortical and Behavioral
842 Responses to Speech Feedback Alterations. *J. Neurosci.* 33, 12090–12098.
843 <https://doi.org/10.1523/JNEUROSCI.1008-13.2013>
- 844 Noble, S., Scheinost, D., Constable, R.T., 2019. A decade of test-retest reliability of functional
845 connectivity: A systematic review and meta-analysis. *Neuroimage* 203, 116157.
846 <https://doi.org/10.1016/j.neuroimage.2019.116157>
- 847 Noble, S., Spann, M.N., Tokoglu, F., Shen, X., Constable, R.T., Scheinost, D., 2017. Influences on the
848 Test-Retest Reliability of Functional Connectivity MRI and its Relationship with Behavioral
849 Utility. *Cereb Cortex* 27, 5415–5429. <https://doi.org/10.1093/cercor/bhx230>
- 850 Oldfield, R.C., 1971. The assessment and analysis of handedness: the Edinburgh inventory.
851 *Neuropsychologia* 9, 97–113.
- 852 Olthoff, A., Baudewig, J., Kruse, E., Dechent, P., 2008. Cortical Sensorimotor Control in Vocalization: A
853 Functional Magnetic Resonance Imaging Study. *The Laryngoscope* 118, 2091–2096.
854 <https://doi.org/10.1097/MLG.0b013e31817fd40f>
- 855 Pando-Naude, V., Barrios, F.A., Alcauter, S., Pasaye, E.H., Vase, L., Brattico, E., Vuust, P., Garza-
856 Villarreal, E.A., 2019. Functional connectivity of music-induced analgesia in fibromyalgia. *Sci*
857 *Rep* 9, 15486. <https://doi.org/10.1038/s41598-019-51990-4>
- 858 Pannunzi, M., Hindriks, R., Bettinardi, R.G., Wenger, E., Lisofsky, N., Martensson, J., Butler, O.,
859 Filevich, E., Becker, M., Lochstet, M., Kühn, S., Deco, G., 2017. Resting-state fMRI
860 correlations: From link-wise unreliability to whole brain stability. *Neuroimage* 157, 250–262.
861 <https://doi.org/10.1016/j.neuroimage.2017.06.006>
- 862 Papitto, G., Friederici, A.D., Zaccarella, E., 2019. The topographical organization of motor processing:
863 An ALE meta-analysis on six action domains and the relevance of Broca’s region. *NeuroImage*
864 116321. <https://doi.org/10.1016/j.neuroimage.2019.116321>

- 865 Power, J.D., Barnes, K.A., Snyder, A.Z., Schlaggar, B.L., Petersen, S.E., 2012. Spurious but systematic
866 correlations in functional connectivity MRI networks arise from subject motion. *Neuroimage*
867 59, 2142–2154. <https://doi.org/10.1016/j.neuroimage.2011.10.018>
- 868 Preibisch, C., Neumann, K., Raab, P., Euler, H.A., von Gudenberg, A.W., Lanfermann, H., Giraud, A.-L.,
869 2003. Evidence for compensation for stuttering by the right frontal operculum. *NeuroImage*
870 20, 1356–1364. [https://doi.org/10.1016/S1053-8119\(03\)00376-8](https://doi.org/10.1016/S1053-8119(03)00376-8)
- 871 Price, C.J., 2012. A review and synthesis of the first 20 years of PET and fMRI studies of heard speech,
872 spoken language and reading. *Neuroimage* 62, 816–847.
873 <https://doi.org/10.1016/j.neuroimage.2012.04.062>
- 874 Primaßin, A., 2019. Longitudinal structural and functional brain changes associated with stuttering
875 improvement by therapy or brain lesion; (Doctoral dissertation). Georg August University,
876 Göttingen.
- 877 Rauschecker, A.M., Pringle, A., Watkins, K.E., 2008. Changes in neural activity associated with
878 learning to articulate novel auditory pseudowords by covert repetition. *Hum. Brain Mapp.*
879 29, 1231–1242. <https://doi.org/10.1002/hbm.20460>
- 880 Riley, J., Riley, G., Maguire, G., 2004. Subjective Screening of Stuttering severity, locus of control and
881 avoidance: research edition. *Journal of Fluency Disorders* 29, 51–62.
882 <https://doi.org/10.1016/j.jfludis.2003.12.001>
- 883 Rödel, R.M.W., Olthoff, A., Tergau, F., Simonyan, K., Kraemer, D., Markus, H., Kruse, E., 2004. Human
884 Cortical Motor Representation of the Larynx as Assessed by Transcranial Magnetic
885 Stimulation (TMS). *The Laryngoscope* 114, 918–922. <https://doi.org/10.1097/00005537-200405000-00026>
- 886
- 887 Rottschy, C., Langner, R., Dogan, I., Reetz, K., Laird, A.R., Schulz, J.B., Fox, P.T., Eickhoff, S.B., 2012.
888 Modelling neural correlates of working memory: a coordinate-based meta-analysis.
889 *Neuroimage* 60, 830–846. <https://doi.org/10.1016/j.neuroimage.2011.11.050>
- 890 Segawa, J.A., Tourville, J.A., Beal, D.S., Guenther, F.H., 2015. The neural correlates of speech motor
891 sequence learning. *Journal of cognitive science* 27, 819–831.
892 https://doi.org/10.1162/jocn_a_00737
- 893 Simonyan, K., 2014. The laryngeal motor cortex: its organization and connectivity. *Current Opinion in*
894 *Neurobiology, SI: Communication and language* 28, 15–21.
895 <https://doi.org/10.1016/j.conb.2014.05.006>
- 896 Simonyan, K., Fuertinger, S., 2015. Speech networks at rest and in action: interactions between
897 functional brain networks controlling speech production. *J. Neurophysiol.* 113, 2967–2978.
898 <https://doi.org/10.1152/jn.00964.2014>
- 899 Simonyan, K., Ostuni, J., Ludlow, C.L., Horwitz, B., 2009. Functional but not structural networks of the
900 human laryngeal motor cortex show left hemispheric lateralization during syllable but not
901 breathing production. *The Journal of Neuroscience* 29, 14912–14923.
902 <https://doi.org/10.1523/JNEUROSCI.4897-09.2009>
- 903 Tourville, J.A., Reilly, K.J., Guenther, F.H., 2008. Neural mechanisms underlying auditory feedback
904 control of speech. *NeuroImage* 39, 1429–1443.
905 <https://doi.org/10.1016/j.neuroimage.2007.09.054>
- 906 Toyomura, A., Fujii, T., Kuriki, S., 2015. Effect of an 8-week practice of externally triggered speech on
907 basal ganglia activity of stuttering and fluent speakers. *NeuroImage* 109, 458–468.
908 <https://doi.org/10.1016/j.neuroimage.2015.01.024>
- 909 Turkeltaub, P.E., Eden, G.F., Jones, K.M., Zeffiro, T.A., 2002. Meta-Analysis of the Functional
910 Neuroanatomy of Single-Word Reading: Method and Validation. *NeuroImage* 16, 765–780.
911 <https://doi.org/10.1006/nimg.2002.1131>
- 912 Vahdat, S., Darainy, M., Milner, T.E., Ostry, D.J., 2011. Functionally Specific Changes in Resting-State
913 Sensorimotor Networks after Motor Learning. *The Journal of Neuroscience* 31, 16907–16915.
914 <https://doi.org/10.1523/JNEUROSCI.2737-11.2011>
- 915 Walsh, B., Tian, F., Tourville, J.A., Yücel, M.A., Kuczek, T., Bostian, A.J., 2017. Hemodynamics of
916 speech production: An fNIRS investigation of children who stutter. *Sci Rep* 7, 1–13.
917 <https://doi.org/10.1038/s41598-017-04357-6>

- 918 Watkins, K.E., Smith, S.M., Davis, S., Howell, P., 2008. Structural and functional abnormalities of the
919 motor system in developmental stuttering. *Brain* 131, 50–59.
920 <https://doi.org/10.1093/brain/awm241>
921 Webster, R.L., 1980. *The Precision Fluency Shaping Program: Speech Reconstruction for Stutterers*.
922 Communications Development Corporation.
923 Webster, R.L., 1974. A behavioral analysis of stuttering: treatment and theory, in: Calhoun, K.S.,
924 Adams, H.E., Mitchell, K.M. (Eds.), *Innovative Treatment Methods in Psychopathology*.
925 Wiley, New York, p. 17–67.
926 Whitfield-Gabrieli, S., Nieto-Castanon, A., 2012. Conn: a functional connectivity toolbox for
927 correlated and anticorrelated brain networks. *Brain Connect* 2, 125–141.
928 <https://doi.org/10.1089/brain.2012.0073>
929 Xue, G., Aron, A.R., Poldrack, R.A., 2008. Common Neural Substrates for Inhibition of Spoken and
930 Manual Responses. *Cereb Cortex* 18, 1923–1932. <https://doi.org/10.1093/cercor/bhm220>
931 Yaruss, J.S., Quesal, R.W., 2014. *OASES: Overall Assessment of the Speaker’s Experience of Stuttering*.
932 Pearson Assessments, Bloomington.
933 Zhang, R., Geng, X., Lee, T.M.C., 2017. Large-scale functional neural network correlates of response
934 inhibition: an fMRI meta-analysis. *Brain Struct Funct* 1–18. [https://doi.org/10.1007/s00429-](https://doi.org/10.1007/s00429-017-1443-x)
935 [017-1443-x](https://doi.org/10.1007/s00429-017-1443-x)
936

937

938 **Acknowledgments**

939 This work was supported by the DFG (SO 429/4-1 to M.S.). We thank Bettina Helten for the co-
940 analysis of the speech samples, Michael Bartl for supporting the organization of the behavioral data,
941 and Britta Perl and Ilona Pfahlert for assistance with the acquisition of the MRI data.

942

943 **Author contributions**

944 AK, AP, PD, WP, MS, and NEN conceptualized and designed the study. AP acquired the data. AK and
945 NEN analysed the rs-fMRI data. AK and NEN interpreted the data, drafted, and revised the
946 manuscript for content. All authors reviewed the manuscript.

947

948 **Additional Information**

949 The author(s) declare no competing interests.

